EYE SHAPE AND PERIPHERAL REFRACTIVE ERROR IN THE DEVELOPMENT OF MYOPIA

A thesis presented to the graduate faculty of
The New England College of Optometry in partial fulfillment
of the requirements for the degree of Master of Science

Kristen Totonelly

April, 2010

©Kristen Totonelly
All rights reserved

The author hereby grants The New England College of Optometry permission to reproduce and to distribute publicly paper and electronic copies of the thesis document in whole or in part.

EYE SHAPE AND PERIPHERAL REFRACTIVE ERROR
IN THE DEVELOPMENT OF MYOPIA

Kristen Totonelly

This manuscript has been read and accepted by the
Thesis Committee in satisfaction of the
thesis requirement for the degree of Master of Science

4-16-10
Date

Nancy J. Coletta
Nancy J. Coletta, OD, PhD
Graduate Faculty Co-Advisor

Jane Gwiazda
Jane Gwiazda, PhD

Chea-su Kee, PhD

David Troilo, PhD
Graduate Faculty Advisor

6-14-10
Date

Nancy J. Coletta
Nancy J. Coletta, OD, PhD
Director of Graduate Studies

The New England College of Optometry

Abstract

EYE SHAPE AND PERIPHERAL REFRACTIVE ERROR IN THE DEVELOPMENT OF MYOPIA

Kristen Totonelly
The New England College of Optometry, 2010

Introduction

Peripheral refractive state and eye shape have been found to differ in humans with differences in axial refractive state, suggesting that they may be factors in the development of axial refractive error. Myopic human eyes have been found to have less myopia peripherally and prolate shape, while hyperopic eyes have less hyperopia peripherally and oblate shape. Whether peripheral refractive state and eye shape influence on-axis refractive state remains unclear. The purpose of this study was to first establish a contact lens rearing paradigm in a primate model of eye growth and then to examine changes in peripheral refractive state and eye shape following induced axial refractive error.

Methods

Juvenile marmoset (*Callithrix jacchus*) monkeys were reared with soft contact lenses for an average duration of 10 weeks. Myopic and hyperopic defocus was imposed with plus lenses (+3 D stepped up to +5 D) and minus lenses (-3 D stepped up to -5 D), respectively. Plano lenses were used as control. Marmosets were reared either monocular or binocularly with contact lenses. Monocular marmosets wore either a plus (n=10) or minus (n=13) lens in one eye and plano lens over the other eye. Binocular marmosets (n=9) wore lenses that were equal in power but opposite sign (±3 D stepped up to ±5 D). Control subjects were untreated (n=11). Refractive state (spherical equivalent refractive error) was measured using

an infrared video refractometer both on-axis and at eccentricities of 20° & 40° along the horizontal meridian. Axial vitreous chamber depth and eye shape were measured using ultrasonography and magnetic resonance imaging (MRI), respectively.

Results

Minus lenses induced axial myopia, significantly longer vitreous chamber depth, prolate shape, and relative peripheral hyperopia. Plus lenses induced axial hyperopia, significantly reduced vitreous chamber depth, oblate shape, and relatively less hyperopia peripherally, compared to minus lens treated marmosets. Binocular lens reared marmosets produced larger interocular differences than monocular lens reared subjects in both refractive state (negative lens-positive lens: -5.72 ± 0.056 D, $p<0.001$) and vitreous chamber depth (0.0275 ± 0.047 mm, $p<0.001$). Marmoset eyes have a nasal-temporal asymmetry in peripheral refraction and shape. The peripheral refractions of myopic eyes were relatively more hyperopic, but only on the nasal side of the retina, corresponding to relatively reduced vitreous chamber depth in that region. The degree of relative hyperopia in the nasal periphery was significantly correlated and inversely proportional to the degree of myopia induced on-axis ($R=0.78$, $p<0.01$). There were no significant differences in peripheral refraction and shape between lens-treated and control eyes in the temporal retina.

Conclusions

Marmosets produce compensatory eye growth and refractive changes for imposed defocus with soft contact lenses. Similar to human myopes, induced axial myopia in marmosets is associated with relative peripheral hyperopia and prolate shape change, but with a nasal-temporal asymmetry.

Acknowledgements

There are many people who I would like to thank and for whom with out their help this work would not have been possible. First off, I want to thank David Troilo, for introducing me to field of myopia, mentoring me over the years, and giving me endless opportunities to further my career in myopia research. I would also like to thank Nancy Coletta, Frances Rucker, and Alexandra Benavente-Perez for their help with revisions and encouraging words.

TABLE OF CONTENTS

Abstract iii

Acknowledgements v

Table of Contents vi

List of Figures viii

Introduction 1

Background 3

Experimental Models of Eye Growth 3

Local Regulation of Eye Growth 5

Peripheral Refraction and Eye Shape 6

MRI and Eye Shape 10

Purpose of Study 13

Methods 15

Subjects 15

Contact Lens Design and Fit 15

Optometric Measurements 16

Magnetic Resonance Imaging (MRI) 18

Statistical Analysis 21

Results.....21

I. Contact-lens rearing.....21

II. Peripheral Refraction.....23

III. Eye Shape.....25

Discussion.....40

References.....46

List of Figures

Figure 1: Ocular structures resolved in MRIs 19

Figure 2: Measurements of eye shape made with *ImageJ* software 20

Figure 3a: Spherical equivalent refractive error compensation to lens wear 27

Figure 3b: Vitreous chamber depth compensation to lens wear 27

Figure 4: Rate of change in vitreous chamber depth 28

Figure 5: Spherical equivalent refractive state and vitreous chamber depth in plano lens treated and untreated eyes 29

Figure 6: Interocular difference in corneal power over the duration of lens wear 30

Figure 7: Example of how peripheral refractive state was visualized 31

Figure 8a: Spherical equivalent refractions of control subjects 32

Figure 8b: Spherical equivalent refractions of the left and right of eyes of control subjects 32

Figure 9a: Relative spherical equivalent refractions of binocular lens reared marmosets 33

Figure 9b: Relative spherical equivalent refractions of monocular lens reared marmosets 33

Figure 10: Linear regressions of relative refractive error off axis versus on axis in minus lens treated eyes 34

Figure 11: Eye shape ratio 35

Figure 12a: Linear regressions of eye shape ratio to contact lens power 36

Figure 12b: Linear regressions of eye shape ratio to axial refractive error 36

Figure 12c: Linear regressions of eye shape ratio to vitreous chamber depth 36

Figure 13a: Vitreous chamber depth measured along the horizontal plane for untreated control eyes 37

Figure 13b: Nasal-temporal vitreous chamber depth differences measured along the horizontal plane for untreated control eyes.....38

Figure 14a: Vitreous chamber depths measured along the horizontal plane for negative lens treated eyes.....39

Figure 14b: Vitreous chamber depths relative to central 20° measured along the horizontal plane for negative lens treated eyes 39

Figure 15: Example of a MRI scan of a binocular lens reared marmoset.....43

Introduction

Myopia results when the eye's axial length exceeds its focal length. The prevalence of myopia has increased substantially over the past decade, affecting approximately 30% of adults in the United States and more than 80% of students in urban East Asia (Vitale, Ellwein, Cotch, Ferrus, & Sperduto, 2008; Lin, Shih, Hsiao, & Chen, 2004). Although the etiology of myopic development is unclear, its progression is thought to be a combination of genetic and environmental factors (Hepsen, Evereklioglu & Bayramlar, 2001). Children, for example, are at a greater risk of developing myopia if either one or both of their parents are myopic, suggesting that myopia is a hereditary (Pacella, McLellan, Grice, Del Bono, Wiggs, & Gwiazda, 1999). Classic twin studies have further demonstrated a genetic component to myopic development (Teikari, O'Donnell, Kaprio, & Koskenvuo, 1980; Hammond, Sneider, Gilbert, & Spector, 2001).

Visual input influences eye growth and the development of refractive state (review: Wallman and Winawer, 2004). Recent findings that myopic prevalence increases in urban environments suggest that environmental stimuli may trigger myopia (Lin et al., 2004). Environmental factors, such as increased amounts of near work and educational level, are thought to contribute to the onset of myopia. The role of near work in myopia was recently investigated in a sample of 12 year-old Australian school children (Ip, Saw, Rose, Morgan, Kifley, Wang, and Mitchell, 2008). Ip et al., 2008 found that children who continuously read (>30 minutes) at a close reading distance (<30 cm) were significantly more likely to have myopia. Interestingly, children who spend more time outdoors are also less likely to develop myopia (Jones, Sinnott, Mutti, Mitchell, Moeshburger, & Zadnik, 2007; Rose, Morgan, Ip,

Kifley, Huynh Smith, & Mitchell, 2008). A study investigating the relationship of outdoor activity and myopia in Singapore teenage children found that children who spent more time outdoors had significantly less myopic refractions and shorter axial lengths relative to children who spent less time outdoors (Dirani, Tong, Gazzard, Zhang, Chia, Young, Rose, Mitchell & Saw, 2009). Dirani et al., 2009 suggest that exposure to sunlight may be a "protective factor" against myopic development by inducing pupil constriction and consequently allowing a larger depth of visual field that diminishes retinal blur.

Neonatal eyes typically go through a period of adjustment, starting out ametropic, and through a visually guided process, move toward emmetropia, called emmetropization. The plasticity of the eye during infancy allows for compensation to visual defocus through mechanisms affecting axial length, including moving the retina toward the image plane, to achieve clear focus (review: Wallman, 1993). Unfortunately, for reasons that are not fully understood, some eyes are unable to achieve emmetropia and instead develop refractive error. Determining how visual experience regulates both eye growth and refractive state may elucidate the problem of myopic development and provide insight on how to stop subsequent progression.

Background

Experimental Animal Models of Eye Growth

Animal models in a variety of species including fish, reptiles, birds, and primates, have been used to study how manipulations of visual experience affects emmetropization and lead to the development of refractive state (Baylor & Shaw, 1962; Weisel & Raviola, 1977; Wallman, Turkel, & Trachtman, 1978; Schaeffel, Glasser, & Howland, 1988; Troilo, Judge, Ridley & Baker, 1990; Troilo & Wallman, 1991; Hung, Crawford, & Smith, 1995). An animal's visual experience may be altered either through form-deprivation or by wearing spectacle or contact lenses, and all methods have repeatedly shown that altering refractive state early in life results in compensatory changes in axial growth. Further suggesting that emmetropization is dependent on the visual environment and when normal visual experience is absent, refractive errors develop.

Form Deprivation

Form deprivation is induced either by placing a diffuser over the eye, or eye-lid suturing, and both techniques produce abnormal visual experience, which the eye compensates to by elongating and developing axial myopia. Studies on the effects of monocular form-deprivation in macaque monkeys, for example, found that eyes lids sutured at birth result in enlarged, myopic eyes (Wiesel & Raviola, 1977). Visual form deprivation has also been found to alter eye shape in a number of species including chicks (Wallman, Turkel, & Trachtman, 1978), tree shrews (Sherman, Norton & Casagrande, 1977; McBrien & Norton, 1992, Norton, Essinger & McBrien, 1994) and monkeys (Wiesel & Raviola, 1977;

Raviola & Wiesel, 1978; Troilo & Judge, 1993; Smith III, Bradley, Fernades & Boothe, 1999). Research shows that form-deprived eyes recover to a state of emmetropia once the deprivation is removed, providing further evidence that visual experience guides ocular growth.

Spectacle and Contact lenses

Postnatal eye growth and development of refractive error depend on the quality of visual input to the eye. Defocusing the optical quality experienced by the retina results in compensatory changes in eye growth so that the retinal image maintains focus along the optical axis (e.g. emmetropia is maintained).

More recently, spectacle and contact lenses have been used to impose varying amounts of retinal defocus and study how the eye compensates for imposed blur during emmetropization (Wallman et al., 1978; Schaeffel, Glasser, & Howland, 1988; Smith, Hung & Harwerth, 1994; Hung, Crawford & Smith, 1995; Whatham & Judge, 2001; Wallman & Winawer, 2004). Specifically, negative lenses impose hyperopic defocus (focus behind of the retina), which the eye compensates for by increasing axial length and thinning the choroid, so that the retina is moved back toward the image plane. Positive lenses impose myopic defocus (focus in front of the retina), which the eye compensates for by slowing axial growth and thickening the choroid, so that the retina is pushed forward to the image plane. Spectacle and contact lens wear in chickens, guinea pigs, tree shrews, and monkeys show that imposed defocus at the fovea affects both eye growth and refractive state, and is used to

guide emmetropization (Wallman et al., 1981; Wallman, 1993; Troilo & Nickla, 2000; Norton, Siegwart & Amedo, 2006).

Although the use of either spectacle and contacts achieve the same end point: altered eye growth and refractive state, soft contact lenses have more recently been used to research emmetropization in animal models. Soft contacts are advantageous over spectacle lenses because they do not restrict the eye's visual field. Initially though, researchers were hesitant to switch to soft contact lenses because of findings in both chickens and primates, that continuous wear of soft contacts resulted in hyperopia due to corneal flattening (Callender & Sivak, 1991; Hung & Smith, 1996). If soft contacts are removed overnight, however, they do not produce flattening of the cornea. Whatham & Judge (2001) raised marmoset monkeys (*Callithrix jacchus*) with extended wear soft contact lenses to determine if limiting the daily duration of lens wear would eliminate the side effects of continuous lens wear. Whatham & Judge (2001) found that overnight lens removal in primates avoided the corneal changes as reported by Hung and Smith (1996).

Local Regulation of Eye Growth

Retinal defocus affects eye growth and refractive state, and most likely guides emmetropization. Studies in chickens suggest that local retinal regions control local eye growth and myopia (Wallman, Gottlieb, Rajaram & Fugate-Wentzek, 1987; Miles & Wallman, 1990; Diether & Schaeffel, 1997). More specifically, chickens raised with partial form deprivation occluders developed vitreous elongation and refractive myopia, but only on the deprived part of the retinal region, while the non-deprived part remained emmetropic

(Wallman et al., 1987). The idea that chick eyes locally compensate for imposed local refractive error was further demonstrated by Miles & Wallman (1990), who raised chickens in low-ceiling environments and found that the chickens compensated for the locally imposed hyperopic refractive error by becoming myopic, but only in the upper visual field. Accordingly, Diether and Schaeffel (1997) raised chickens with hemi-field spectacle lenses and found that chick eyes elongated and became myopic, but only in the part of the eye with imposed hemi-field defocus, the other half of the eye remained normal. Similar findings have also been reported in monkeys (Smith, Huang, Hung, Blasdel, Humbird, & Bockhorst, 2009). These results are evidence for local compensatory eye growth to imposed defocus and are further supported by findings that optic nerve sectioning does not prevent compensation for imposed myopic defocus, suggesting that the mechanisms affecting eye growth are regulated both independent of the brain and to locally within the eye (Wildsoet & Wallman, 1995). These findings also suggest that local regulation of ocular growth is dependent on visual experience and may help explain why refractive error varies across the retina.

Peripheral Refraction and Eye Shape

Humans show differences in peripheral refraction at various degrees of eccentricity relative to central refractive state (Ferree & Rand, 1933; Hoogerheide, Rempt & Hoogenboom, 1971; Rempt, Hoogerheide & Hoogenboom, 1971; Millodot & Lamont, 1974). Studies on human peripheral refraction report an increase in peripheral hyperopia relative to the degree of central myopia. More specifically, people who have higher amounts of central myopia also have higher amounts of peripheral hyperopia, whereas individuals

with central hyperopia also have higher amounts of peripheral myopia (Millodot, 1981, Mutti, Sholtz, Freidman, & Zadnik, 2000; Atchison, Seidemann, Schaeffel, Guirao, Lopez-Gil & Artal, 2002; Pritchard & Schmid, 2006).

Peripheral asymmetries have been found in the peripheral refractions of monkeys. A study by Hung, Ramamirtham, Huang, Qaio-Grider, & Smith (2008), measured peripheral refractions in normal infant rhesus monkeys and reported nasal-temporal and superior-inferior asymmetries. The superior and temporal fields were found to have similar refractions as those refractions measured on-axis, but the nasal and inferior fields exhibited more myopia relative to central refractions. Interestingly, the amount of myopia found on the nasal field increased with the degree of central hyperopia.

It has been suggested that peripheral refractive state is related to eye shape (Stone & Flitcroft, 2004; Wallman & Winawer, 2004; Atchinson, Pritchard, Schmid, Scott, Jones & Pope, 2005). Myopic eyes tend to be prolate in shape (longer axial length than equatorial diameter) such that the peripheral retina lies in front of a sphere having the same overall axial length. If the best focal plane of the eye lies on a sphere through the fovea (Stone & Flitcroft 2004; Atchinson et al., 2005), the steep peripheral retinal contour in the myopic eye will result in relative peripheral hyperopia. The eye may compensate for peripheral hyperopia by increasing axial elongation, which in turn creates central myopia. Hyperopic eyes, on the other hand, tend to be oblate in shape (shorter axial length than equatorial diameter) such that the peripheral retina lies behind a sphere having the same overall axial length. The flat peripheral retinal contour in the hyperopic eye will result in relative peripheral myopia, which the eye may compensate for by slowing axial growth. Thus, peripheral refractive error

may be the stimulus for compensatory changes in eye shape, if the area of the retina used to detect defocus during eye growth is located in the periphery. If peripheral refractive error is the stimulus for axial eye growth, then greater hyperopia peripherally will result in greater axial growth that makes the eye more prolate (Stone & Flitcroft, 2004). Alternatively, greater myopia peripherally will result in less axial growth and an oblate shape with the eye being wider than long (Stone & Flitcroft, 2004). Further study of peripheral refraction is needed as it may help explain why some people progress in the development of axial refractive error even after correction.

Peripheral refraction may also alter the rate at which the eye grows and consequent myopic progression. Studies looking at measures of refractive error, axial length, and relative peripheral refractive error before and after the onset of myopia in children, found that children with relative peripheral hyperopia developed axial myopia at a faster rate than children with relative peripheral myopia (Mutti, Hayes, Mitchell, Jones, Moeschberger, Cotter, Kleinstein, Manny, Twelker & Zadnik, 2007). Children with relative peripheral hyperopia also had ocular characteristics as expected with axial myopia: longer vitreous chambers, flatter crystalline lenses, and steeper corneas (Mutti, Sholtz, Friedman & Zadnik, 2000). Similarly, Hoogerheide et al., (1971) studied the pattern of peripheral refraction in young air force pilots, and found that emmetropic pilots who exhibited hyperopic peripheral refractions upon initial examination were more likely to develop central myopia than emmetropes with myopic peripheral refractions. The results of these studies suggest that the pattern of peripheral refraction can influence axial refractive development and should be

further studied, as the pattern of peripheral refraction may predict future shifts in central refraction.

Does peripheral retinal defocus affect eye growth and refractive development?

Recent findings from non-human primates suggest that peripheral vision does affect the process of emmetropization. Form deprivation of the peripheral retina, for example, produced foveal myopia in macaques (Smith, Kee, Ramamirtham, Qiao-Grider & Hung, 2005). A study by Smith et al., (2005) examined how peripheral vision influences eye growth in infant monkeys. Smith et al., (2005) raised infant macaques with diffusers that had small central openings (4-8mm) so that the monkey experienced clear central vision but form deprived peripheral vision, and found that peripheral form deprivation resulted in accelerated axial growth. Smith et al., (2005) then tested if the form-deprived eyes could recover from the induced axial myopia if the eyes were allowed only peripheral vision. The monkeys had the foveae ablated in order to isolate the periphery and the eyes were able to recover. The results of this study have two important implications for the process of emmetropization in primates (1) peripheral deprivation affects central refractive development and (2) an intact fovea is not necessary for emmetropization to occur.

The finding that peripheral refraction affects central refractive development may, however, only occur in primates with foveal vision. A study on chickens, for example, found that peripheral defocus does not necessarily affect central refractive development (Schippert & Schaeffel, 2006). Schippert and Schaeffel (2006) raised chickens with spectacle lenses (+/-7 D) that had central openings (4-8mm) to allow unobstructed central vision. Unlike the

macaque monkeys of Smith et al's., (2005) experiment, chickens with peripheral defocus and clear central vision did not develop axial myopia. Interestingly, the chickens were able to respond to changes in peripheral defocus without changing their central refraction. Schippert and Schaeffel (2006) suggest, however, that because chickens do not have a fovea, but rather an "area centralis," the area of clear central vision may have been too large (>4mm) to properly limit defocus solely to the peripheral visual field. Furthermore, the investigators suggest that, had the chickens been reared with lenses that provided peripheral defocus but with smaller central visual fields (<4mm), axial myopia may have resulted. In accordance, chickens reared with spectacles (+10 D) with plano central zones of 3mm, emmetropized and became hyperopic on-axis (Morgan & Ambadenyia, 2006). Schippert and Schaeffel (2006) suggest that there is a "critical size", 3mm or less, of central vision needed for chickens to respond on-axis to peripheral defocus.

Thus, peripheral refractive error affects the development of central refractive error. Whether peripheral refractions are a cause or consequence of central refractive error remains unclear and further investigation into the development of peripheral refraction is needed.

Magnetic Resonance Imaging (MRI) and eye shape

MRI has been used to reconstruct three-dimensional (3-D) images of the eye and since it allows for analysis along any desired meridian, is an ideal technology to use when investigating the ocular shape of emmetropic, hyperopic, and myopic eyes. Only a few studies have analyzed eye shape with MRI technology and the findings are inconsistent. Cheng, Singh, Kwong, Xiong, Woods & Brady (1992) conducted one of the first MRI

studies, and analyzed eye shape by taking measures from the sclera edge along three ocular dimensions: axial (anterior-posterior), equatorial (nasal-temporal), and vertical (superior-inferior). Cheng et al. (1992), found no difference in shape between emmetropic and hyperopic eyes, both eyes were found to have significantly longer equatorial diameter than either axial or vertical diameters, and the axial and vertical diameters were equal. Myopic eyes were found to be significantly larger than hyperopic and emmetropic eyes, but they were larger in every dimension measured. More specifically, myopic eyes were longer equatorially than axially and longer axially than vertically. These results show that hyperopic, emmetropic, and myopic eyes share a similar "spheroelliptical" shape (wider than long). Furthermore, Cheng et al. (1992), suggest that during myopic progression an overall enlargement or volume expansion occurs. The findings of Chau et al. (2004), however, did not find a relationship between volume of the orbit and either the volume or axial length of the eye, suggesting that the enlarged myopic eye as reported by Cheng et al. (1992) does not result from volume expansion.

In addition to the finding that myopic eyes are longer than emmetropic eyes in the axial, vertical, and horizontal meridians, Atchinson et al. (2004) suggest that the meridians of myopic eyes elongate in different proportions. More specifically, measures of axial length (cornea to retina), height and width (both retina to retina) were measured from MRI scans of emmetropic and myopic eyes. Myopic eyes were found elongated most in the axial direction, less in the vertical direction and least in the horizontal direction. The variance in dimensions of myopic eyes, with horizontal length being shortest, could be due to constraint of the orbit walls. The equatorial growth of an eye may be restricted because the walls of the orbit are

closer to the sides of the eye than behind the eye, resulting in elongated axial length. (Atchinson et al., 2004)

Although previous findings of MRI studies suggest a difference in the dimensions of myopic eyes, the question of how eye shape changes during the development of myopia remains unclear. More recently, 3-D reconstructions of MRIs have been used to better understand the etiology of refractive error. It has been hypothesized that the observed shifts in peripheral refractive state from central refractive state, in myopic and hyperopic eyes, may be due to variances in shape of the posterior globe (Atchinson et al., 2004; Atchinson et al., 2005). Emmetropic eyes are thought to have a spherical shaped posterior globe, having an image shell that directly overlaps a spherical retinal contour, which maintains similar central and peripheral refractive states. The retinal contours of myopes (steeper, longer: prolate posterior globes) and hyperopes (flatter, wider: oblate posterior globes) are thought to cause an offset in alignment between the image shell and retinal contour in the periphery, and explain variances in peripheral refractive state. (Chen, Elsner, Burns, Hansen, Lou, Kwong, & Fulton, 1992; Stone & Flitcroft 2004)

Singh, Logan, & Gilmartin (2006) developed a novel methodology to study the shape of the posterior globe. Briefly, 3-D surface models of eyes were reconstructed from MRIs and color-coded so that variances in sphericity and volume could be visualized. The posterior globe was measured by a comparison of axial length measures to equivalent spherical radius. The 3-D surface reconstructions indicated difference in ocular shape and size among subjects and further suggested that their modeling technique could empirically test for variance in posterior global shape. Thus, a follow-up study (Gilmartin, Logan, & Singh, 2007) used the

3-D modeling technique to study eye shape of aniso- and isometropic subjects and to determine if the eye conformed to a posterior global shape. The results of the study suggest variations in posterior globe conformation between subjects. Emmetropes and myopes were found to maintain a conformation to oblateness and prolateness respectively. These findings, however, contradict an earlier study by Atchinson et al. (2005), who also measured posterior shape from MRIs, but instead of modeling the posterior globe based on a spherical shape, used an ellipsoid shape, and found myopes to be oblate.

The findings from MRI studies are conflicting, but suggest that shape differences between emmetropic, myopic, and hyperopic eyes exist and may explain the etiology of refractive error. A better understanding of the development of myopia could be achieved with a longitudinal study in which eye shape is studied over time and with the progression of myopia. Animal models of myopia are therefore ideal because they allow for controlled visual manipulations of refractive state and easy tracking during a longitudinal study. Non-human primates, marmosets in particular, are ideal subjects of study due to their rapid development of high optical quality eyes, which can be used as a model for human refractive development (Troilo et al., 2000). The small size of marmosets also allows ease in handling, and more importantly, the ability to conduct an experiment in which visual conditions can be manipulated with contact lens wear.

The purpose of this study was to (1) investigate the development of refractive error both on-axis and off-axis in the marmoset monkey, *Callithrix Jacchus*, with the use of soft-contact lenses and (2) explore changes in eye shape during the development of refractive error with the use of magnetic resonance imaging (MRI). In doing so, we hoped to establish

an effective soft contact lens rearing paradigm in marmosets and also explore how changes in peripheral refraction and eye shape following induced refractive error may be involved in the visual regulation of eye growth.

Materials and Methods

Subjects

Marmosets (*Callithrix jacchus*) were housed at The New England College of Optometry. Artificial lighting was provided by daylight-balanced fluorescent lamps (Vita-Light, Fairfield, NJ) on an 8-hour light-16-hour dark cycle (8:00-16:00h). Food and water were supplied ad libitum. All of the rearing and experimental procedures were approved by The New England College of Optometry Institutional Animal Care and Use Committee and were in compliance with the ARVO Statement for the Care and Use of Animals in Research.

Thirty-two marmosets (*Callithrix jacchus*) were obtained at an average age of 76 days (range 41-101) and reared with soft contact lenses for an average duration of 10 weeks (range 6-17). Experimental marmosets wore a positive (n= 10) or negative (n=13) contact lens over one eye (±3 stepped up to ±5D) and a plano lens (0D) in the fellow eye (monocular lens condition). Another group of experimental animals (n=9) wore a positive lens over one eye and a negative lens of equal but opposite power (±3 stepped up to ±5D) in the fellow eye (binocular lens condition). Untreated animals (n=11) provided normal control data (control eyes).

Contact lens design and fit

Contact lenses were custom designed by Innovations in Sight, Inc (Front Royal, VA). Lenses were manufactured with 76% water content, central thickness of 0.12-0.16 mm, base curvatures of either 3.8 or 4.0 mm and a lens diameter of 6.5 mm. Lenses were fit to approximately 10% flatter than the corneal curvature measured with infrared video

keratometry. Marmosets wore contacts for the complete duration (8 hrs) of the light cycle. For lens insertion and removal, a method developed by Whatham & Judge (2001) was adopted. Briefly, the marmoset was removed from their home cage and restrained in a primate-chair. First, a custom-made lid retractor was inserted to keep the eyelids apart. Next, the investigator stabilized the marmoset's head with one hand and used the other hand to insert the lens using a pair of plastic tip forceps. Special care was taken so that the lid-retractor or forceps never directly touched the cornea. Once the lens was inserted, the lid retractor was removed, and the eye was gently massaged to remove any air bubbles under the lens. The marmoset was then returned to their home cage, the lights were turned on, and lenses remained in place for an 8-hour light cycle. The investigator periodically checked the cage (every 2 hours) for any lost lenses. Approximately 4 hours after insertion, the marmoset was refracted daily on a Power refractor (MultiChannel Systems, Germany) in full refraction mode to insure that the lenses were in place. If a lens was lost it was replaced immediately. For contact lens removal, marmosets were removed from their home cages, hand held by the investigator, and lenses were removed by gently pushing in a down and upward motion (with two fingers) on the upper and lower lids. Once the lens was removed, it was cleaned and stored in saline solution (Opti-One No Rub), and the marmosets was returned to their cages with the lights turned off.

Optometric Measurements

On –axis refractive state, corneal curvature, and vitreous chamber depth

A complete cycloplegic exam, as previously described by (Troilo, Nickla & Wildsoet, 2000a), was performed prior, during (every 3 weeks) and following the period of lens wear. Briefly, 1 hour before measurements, contacts were removed, stored in saline solution, and 2 drops (given 5 minutes apart) of 1% cyclopentolate were topically administered into each eye. This allowed for maximal levels of cycloplegia during the exam (Boisvert, Wildsoet & Troilo, 1998). On-axis refractometry was performed first, using an Infrared PowerRefractor (MultiChannel Systems, Germany) in the full refraction mode calibrated for marmosets. The marmoset was hand-held by the investigator so that its' head was stabilized and remained in focus on the camera at a 1 m working distance. Next, an infrared Keratometer was used to reliably measure corneal curvature. The marmoset was then anesthetized with an intramuscular injection of Alfaxan (0.15 mg/kg). Refractive state was measured next by streak retinoscopy and then with a Hartinger Coincidence Refractometer (Carl Zeiss, Oberkochen, Germany). All axial refraction data presented are the means of the refractometry and retinoscope data expressed as the spherical equivalent refractive error.

Vitreous chamber depth was measured by high-frequency A-Scan ultrasonography (Troilo, Nickla, & Wildoset, 2000). The anesthetized marmoset was aligned with the A-scan probe so that the echoes of the cornea, lens, and retina were maximized, insuring alignment along the optical axis. Vitreous chamber depth was calculated from the average of at least 8 separate measurements using the velocity of sound in the vitreous chamber (1.534 m/sec). (Troilo, Nickla & Wildsoet, 2000b)

Off-axis refractions

Refractive state was measured using the PowerRefractor (MultiChannel Systems, Germany) in the full refraction mode calibrated for marmosets. Following cycloplegia, marmosets were hand held by the investigator 1m from the PowerRefractor. Throughout data collection, marmosets were conscious and cyclopleged. The investigator hand-held the marmoset, stabilizing the marmoset's head position, while the marmoset had free range of visual gaze. In order to get measures of off-axis refractions, the investigator slowly rotated the marmoset's head back and forth throughout data collection. The power refractor reliably captured out to ±40 degrees along the horizontal gaze position, data from vertical gaze position were not analyzed. Data for analysis were collected ±1 degree at 0, 20 and 40 degrees eccentricities and are expressed as the mean spherical equivalent refractive error.

Magnetic Resonance Imaging (MRI)

Image acquisition

MR imaging was acquired on a 4.7 tesla magnet with a Brucker Biospec console running Paravision 3.2 software. Prior to the start of the scan, marmosets were anesthetized with an intramuscular injection of Alfaxan (0.20ml/100g). Subject's heart rate and blood oxygen levels were monitored with the use of a pulse-oximeter. Once fully anesthetized, the marmoset was positioned supine on a custom-made animal bed and a 200 MHz surface coil (3.5 cm radius) was placed over the marmoset's face. The marmoset was then loaded into the scanner so that it's head was centered in the transmit coil (72 mm diameter). Once the marmoset was loaded into the scanner, a tripilot imaging sequence was used to access eye

position and adjust slice orientation. The orientation of the slice was adjusted so that the apex of the cornea, pupil opening, lens, and optic nerve would be imaged (Figure 1).

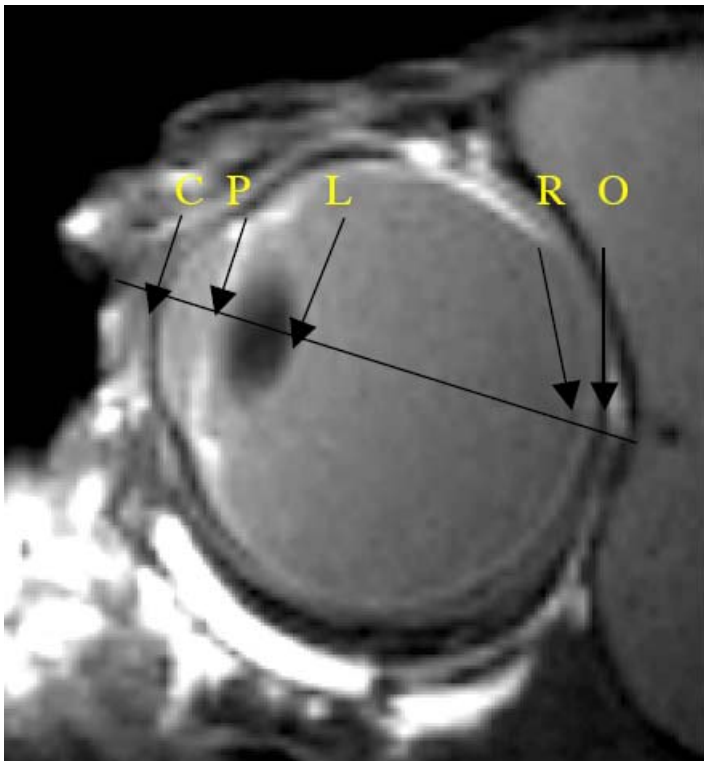


Figure 1. Image acquired from tripilot scan depicting optimal slice orientation (black line). Structures resolved include the apex of the cornea (C), pupil opening (P), lens (L), Retina (R), optic nerve (O).

Next, a T1 weighted multislice spin-echo (MSME) sequence was performed. Scan time took approximately 15 minutes and consisted of a total of 10 slices with 1 mm thickness; TR = 600 ms; TE = 11 ms; flip angle=180 degrees, NEX=16. Image resolution was 700 μm with an Acquisition matrix = 128 x 128 pixels and a FOV= 2.56 cm.

MR Image Analysis

Axial eye length and shape were measured from MRIs sliced through the center of the eye in the transverse (horizontal) sections following lens wear. MRIs were analyzed with ImageJ 1.4 software. For each eye, the slice with the largest axial diameter was used for analysis. The ratio of the equatorial diameter (EQ) to the depth of the vitreous chamber (VC) measured along the anterior-posterior (AP) axis was used as a simple measure of eye shape (Totonelly & Troilo, 2007). The AP axis was determined with the use of an ImajeJ macro, which fit a line to the center of curvatures of the anterior corneal surface and the anterior posterior lens surfaces. The EQ of the eye was taken as the distance from retina to retina of a line orthogonal to the AP axis at its midpoint through the eye from cornea to retina. Vitreous chamber depths across the retina were measured every 10° (± 90°) from the apex of posterior lens surface, starting at the nasal retinal edge and ending temporally (Figure 2).

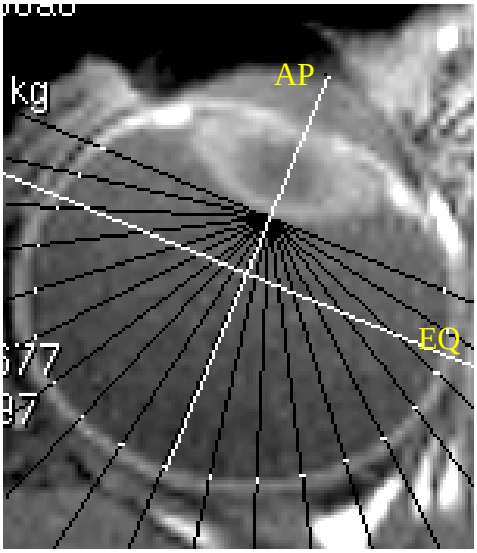


Figure 2. Measurements of eye shape made with *ImageJ*. Black lines represent vitreous chamber depths measured every 10 degrees (± 90°). Vertical and horizontal white lines depict the anterior-posterior (AP) axis and equatorial diameters (EQ) respectively.

Statistical Analysis

Unpaired student t-tests were used to determine an effect of contact lens wear. ANOVAs (repeated- measures) were then used to determine whether there were differences in axial refractive state, vitreous chamber depth, and peripheral refractive state. Linear regression and Pearson Correlations were also used to analyze the relationship between the power and sign of contact lens worn, to the on-axis refractive state, peripheral refractive state, and EQ/VC shape ratio.

RESULTS

I. Contact-lens rearing (Troilo, Totonelly, and Harb, 2009)

Marmosets reared with contact lenses produce compensatory changes in axial growth and refractive state (Figure 3). Figure 3A shows the changes over time in vitreous chamber depth (left) and refractive error (right). For eyes wearing monocular positive lenses the vitreous chambers became relatively smaller than their contralateral controls (top left), and their refractive state shifted toward hyperopia (top right). For eyes wearing monocular negative lenses, the eyes became relatively longer than their contralateral controls (top left, middle) and their refractive state shifted towards myopia (top right, middle). Of note, eyes wearing binocular lenses showed a larger response for both the difference in axial length (top left, bottom) and for refractive errors (top right, bottom).

Figure 3B shows the individual refraction and vitreous chamber depth difference data at the end of the lens-rearing period. Eyes wearing monocular negative lenses became significantly myopic (Figure 3B, right: -2.41 ± 0.64 D, $p < 0.01$**)** and had longer vitreous

chamber depth **(**Figure 3B, left: 0.170 ± 0.28 mm, p<0.05**)** relative to controls, while monocular positive lens wear resulted in hyperopic refractive state **(**1.40 ± 0.43 D, p<0.05**)** and shorter vitreous chamber depth **(**-0.082 ± 0.029 mm, p<0.05**)** relative to controls. It is apparent here that marmosets reared with binocular lenses of equal power but opposite sign had the largest interocular differences in both refractive state ("+/-": negative lens-positive lens: -5.72 ± 0.056 D, p<0.001) and vitreous chamber depth (0.275 ± 0.047 mm, p<0.001**)**.

Accordingly, the rate of compensation to the imposed defocus differed between experimental groups (Figure 4). Marmosets wearing binocular lenses of opposite sign had the fastest rate of interocular change in vitreous chamber depth (right bar), while monocular positive lens wear (middle bar) had the slowest (ANOVA, p< 0.05). Of note, the monocular negative lens reared marmosets (left bar) had faster interocular changes in vitreous chamber depth than monocular positive lens reared marmosets (middle bar) (ANOVA, p< 0.05).

In order to confirm that soft contact lens wear, regardless of the power of the lens worn, did not effect eye growth or refraction, a comparison of refractive state and vitreous chamber was performed on plano lens reared and untreated marmosets (Figure 5). There was no significant difference in plano versus untreated control marmosets in terms of either refractive state (Figure 5, left: mean ±SE; 0.25 ± 0.42 vs. 0.06 ± 0.48 D; p= 0.07) or axial vitreous chamber depth (Figure 5, right: 6.53 ± 0.10 vs. 6.39 ± 0.12 mm; p= 0.40). Soft contact lenses also had no significant effect on average corneal power in any of the experimental groups (Figure 6, ANOVA's, p> 0.05).

II. Peripheral Refraction

The pattern of peripheral refraction was visualized by plotting the spherical equivalent refractive error, normalized to the central refractive state, along the horizontal meridian (Figure 7). The mean spherical equivalent refractive state at various eccentricities (0°, ±20°, ±40°) was statistically analyzed.

Controls

There was no significant difference in the pattern of peripheral refractive error in untreated controls (Figure 8, ANOVA, $p > 0.05$). Figure 8a shows the mean spherical equivalent refractive state plotted along the horizontal gaze in untreated marmosets. Although the mean spherical equivalent refractions in untreated control eyes tended toward less hyperopia in both the temporal and nasal retinas (mean ± se, 1.15 ± 0.08 D vs. 1.17 ± 0.04 D) relative to on-axis (1.52 ± 0.40 D), it did not vary significantly as a function of eccentricity (out to ±40°). Accordingly, there was no significant difference in peripheral refractive error between eyes of untreated controls (Figure 8b).

Binocular lens-reared marmosets

Nasal-temporal asymmetries were found in the pattern of peripheral refractions in the eyes of marmosets wearing binocular contact lenses (Figure 9). Figure 9a shows the relative refractive state measured along the horizontal meridian for the plus and minus lens treated eyes of binocular lens reared marmosets, along with untreated control eyes. Both lens treated and untreated control eyes appear to shift towards less hyperopia in the temporal retina (-20°

and -40°) relative to the on-axis refractive state, but neither the minus lens treated or plus lens treated refractive state differed significantly from controls in the temporal retina (ANOVA, $p > 0.05$). It is apparent here that only the negative lens-treated eyes were significantly different from controls in the nasal retina (+20° and +40°), where they were relatively hyperopic (0.98 ± 0.40 and 0.94 ± 0.46, $p<0.01$).

Monocular lens-reared marmosets

Nasal-temporal asymmetries were found in the pattern of peripheral refractions of monocular lens-reared marmosets. Figure 9b shows the relative refractive state of monocular negative and positive lens reared marmosets with contralateral plano control eyes. Similar to binocular lens reared marmosets, the relative off-axis refractive state measured along the temporal retina did not differ between experimental and control eyes (ANOVA, $p > 0.05$). Only the refractive state in the nasal retina (+20° and +40°) differed significantly relative to on-axis, where monocular negative lens treated eyes were significantly hyperopic relative to on-axis refractive state (ANOVA, $p < 0.05$).

Negative lens-reared marmosets

The degree of relative hyperopia for all minus treated eyes (both binocular and monocular lens reared groups) in the nasal retina (+20° and +40°) was significantly correlated and inversely proportional to the degree of myopia induced on-axis, such that greater myopic refractive error measured on- axis corresponded to greater relative hyperopia

measured off-axis at both +20° (Figure 10, left: $r= 0.67$, $p< 0.01$) and +40° (Figure 10, right: $r= 0.63$, $p< 0.01$) in the nasal retina.

III. Eye Shape

Marmoset eyes change shape during the development of induced axial refractive errors (Figure 11). The shape ratio of equatorial diameter to axial vitreous chamber depth (EQ/VC) of control eyes (left) corresponded to an oblate shape (wider-than-long). Relative to controls, eyes wearing negative lenses (middle) became relatively more prolate in shape (longer- than-wide), while eyes wearing positive lenses (right) became more oblate in shape.

Figure 12 shows linear regression plots of the eye shape ratio significantly correlating shape to the power of the contact lens worn (Figure 12a, $r= 0.59$), induced axial refractive error (Figure 12b, $r= 0.45$) and vitreous chamber depth (Figure 12c, $r= 0.40$). Prolateness of eye shape increased with greater negative lens power (Figure 12a), greater axial myopic refractive error (Figure 12b) and longer vitreous chamber depths (Figure 12c). Oblateness of eye shape increased with greater positive lens power (Figure 12a), greater axial hyperopic refractive error (Figure 12b) and shorter vitreous chamber depths (Figure 12b).

Marmoset eyes were found to naturally have some asymmetry is eye shape. The shape ratio of equatorial diameter to axial vitreous chamber depth was found to be greater than 1 for all untreated control eyes, suggesting that marmoset eyes are normally oblate in the horizontal plane. A plot of the mean vitreous chamber depth along the horizontal plane also suggests nasal-temporal asymmetry among untreated control eyes (Figure 13a). Figure 13b shows that in the far periphery (>40 degrees) of untreated control eyes, the nasal side of the

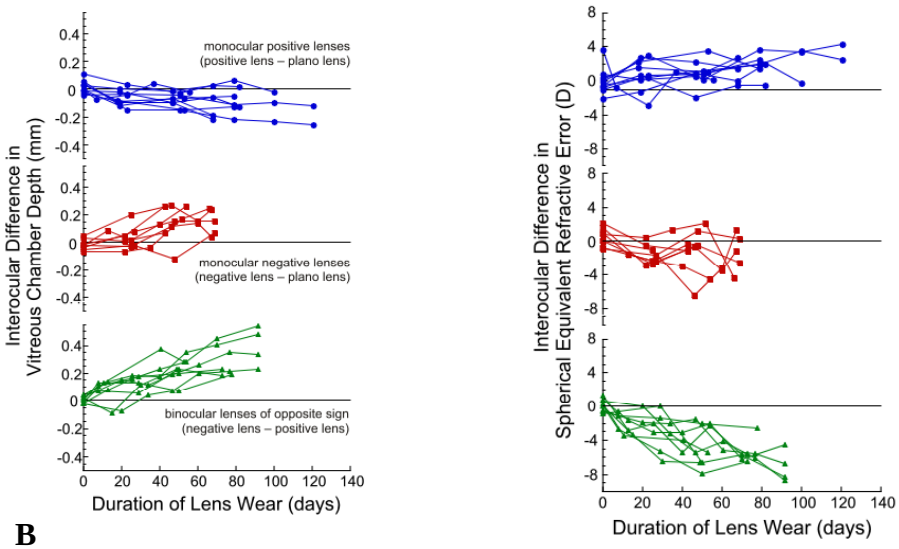
vitreous chamber is deeper than in the central-near periphery (10-40 degrees) where the temporal side is deeper.

Nasal-temporal asymmetries were exaggerated by lens wear. Figure 14a shows the nasal-temporal asymmetry of vitreous chamber depth in lens-treated eyes. The vitreous chamber depth for both positive and negative-lens-treated eyes appears shallower in the nasal periphery (20-40 degrees) than along either the central 20 degrees or temporal 20-40 degrees. Interestingly, when the mean vitreous chamber depth is adjusted relative to the central 20 degrees, the nasal vitreous chamber depth in negative-lens-treated eyes is significantly shallower than in positive-lens-treated eyes (Figure 14b, mean ± SE: -0.38 ± 0.05 mm vs. -0.23 ± 0.04 mm, $p<0.05$).

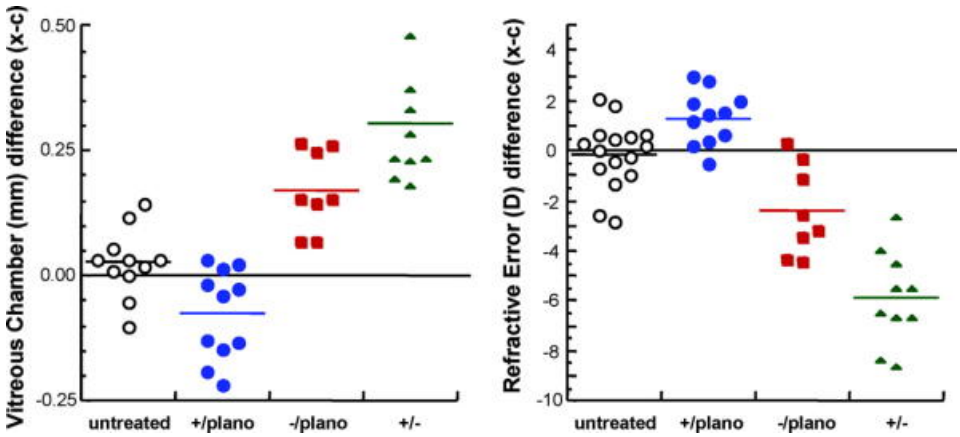
As previously mentioned above, relative to on-axis refractions, off-axis refractive state measured along the nasal retina in negative-lens treated eyes was significantly more hyperopic than in either positive-lens treated or control eyes (Figure 13 & Figure 14). Change in eye shape with induced axial myopia increases nasal-temporal asymmetry (shorter nasal vitreous chamber depth) and corresponds to the relative hyperopia observed in the nasal retina.

Figure 3

A

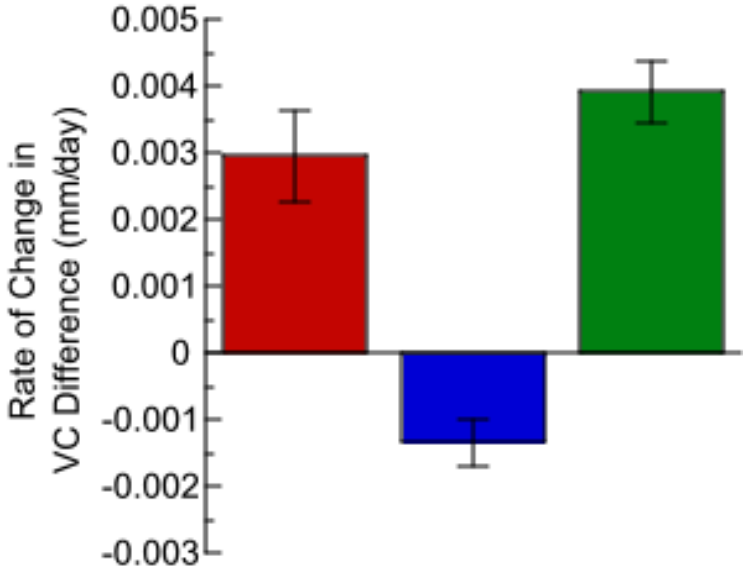


B



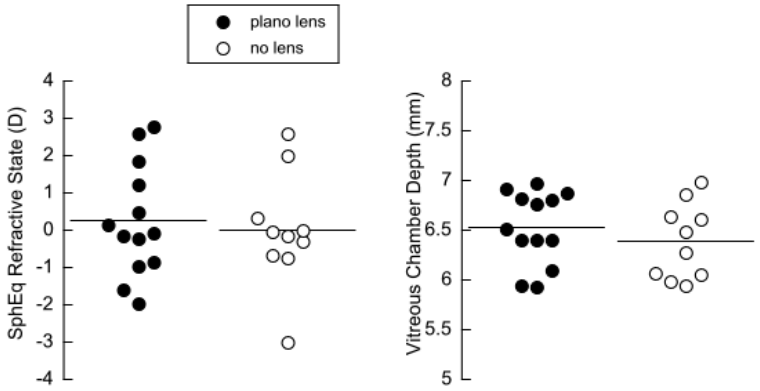
3a. Interocular differences over the duration of lens wear in vitreous chamber depth (top left) and spherical equivalent refractive error (top right) in monocular positive lens reared group (squares), monocular negative lens reared group (circles), and binocular lenses of opposite sign group (triangles). **3b** At the end of lens wear, eyes produced compensatory changes in vitreous chamber depth (left) and refractive error (right). Open circles represent interocular differences (right eye-left eye) of untreated marmosets. Solid circles show interocular differences (experimental-control) from monocular positive lens reared marmosets. Squares show interocular differences (experimental-control) from monocular negative lens reared marmosets. Triangles represent interocular differences (right eye-left eye) from marmosets reared binocularly with lenses of opposite sign. Reproduced with permission, Troilo et al., 2009 ©Lippincott Williams & Wilkins.

Figure 4



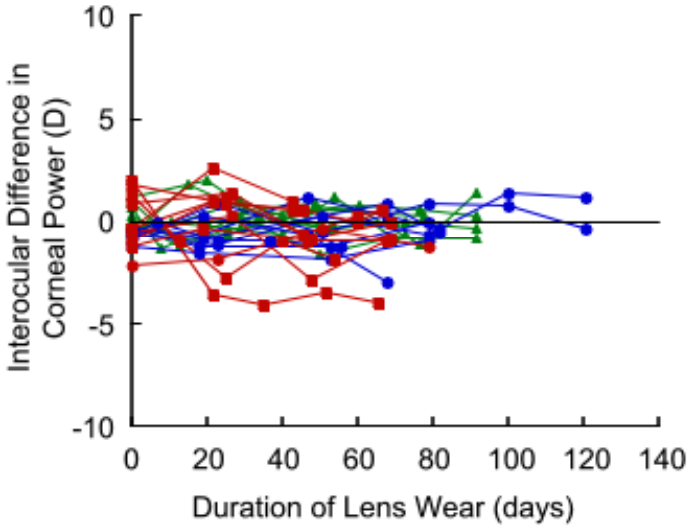
4. The rate of change in vitreous chamber depth differed between experimental groups. Left bar shows the mean interocular change in monocular minus lens treated marmosets. Middle bar shows the mean interocular change in monocular positive lens treated marmosets. Right bar shows the mean interocular change in binocular treated marmosets with lenses of opposite sign. Error bars represent standard error. Reproduced with permission, Troilo et al., 2009 ©Lippincott Williams & Wilkins.

Figure 5



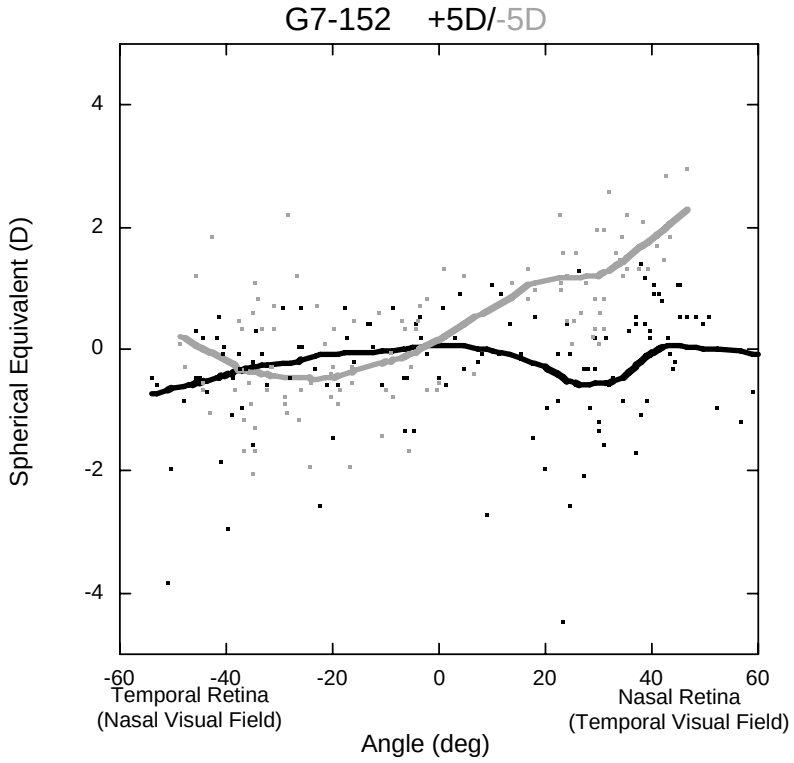
5. Spherical equivalent refractive state (left) and vitreous chamber depth (right) in plano lens treated eyes (black circle) and untreated eyes (white circles). Soft contact lens wear had no affect on the refractive state or vitreous chamber depth in either untreated eyes or plano contact lens treated eyes. There were no significant differences between untreated eyes and plano contact lens treated eyes at the end of lens rearing period.

Figure 6



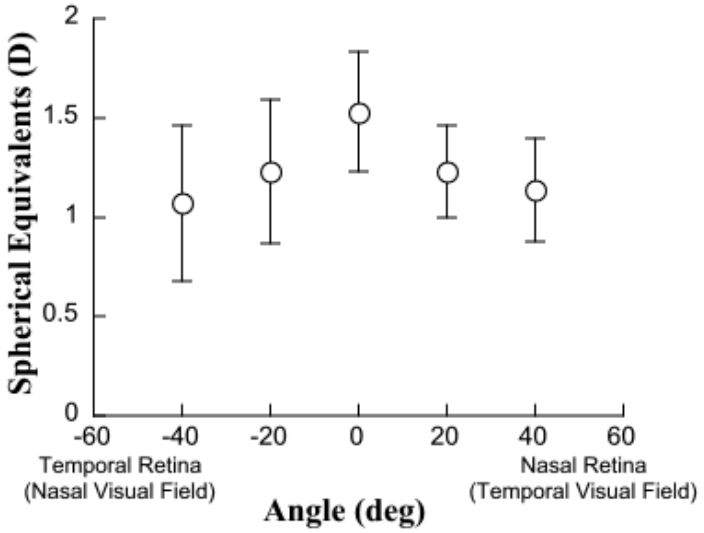
6. Contact lens wear had no effect on the average corneal power throughout the duration of lens wear in any of the experimental groups. Monocular minus lens treated (squares), monocular plus lens treated (circles), binocular treated marmosets with lenses of opposite sign (triangles).

Figure 7



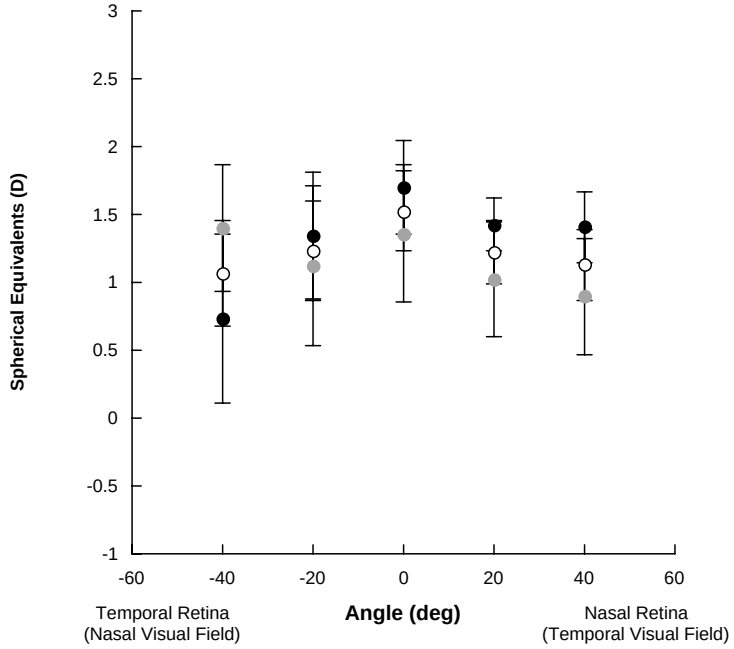
7. Example of how peripheral refractive state was visualized. Data plotted here are the spherical equivalent refractive error measured along the horizontal meridian, normalized to central refractive state, at the end of contact lens rearing for a marmosets reared binocularly with +5/-5 D lenses. Black dots represent data from the eye treated with +5 D lens, fitted with a 33% lowess weighted regression (black solid line). Grey dots represent data from the eye treated with -5 D lens, fitted with a 33% lowess weighted regression (grey solid line).

Figure 8
A



8a. Mean spherical equivalent errors plotted as a function of horizontal eccentricity for control subjects. Bars represent standard error.

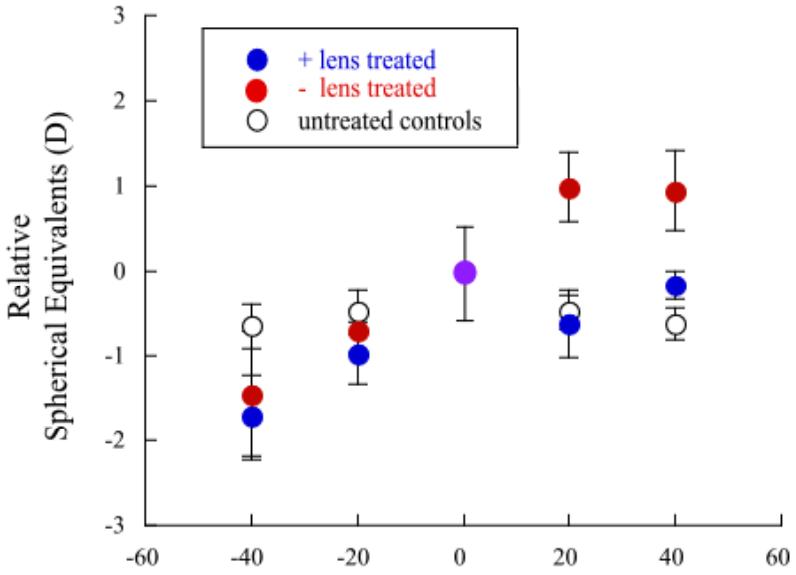
B



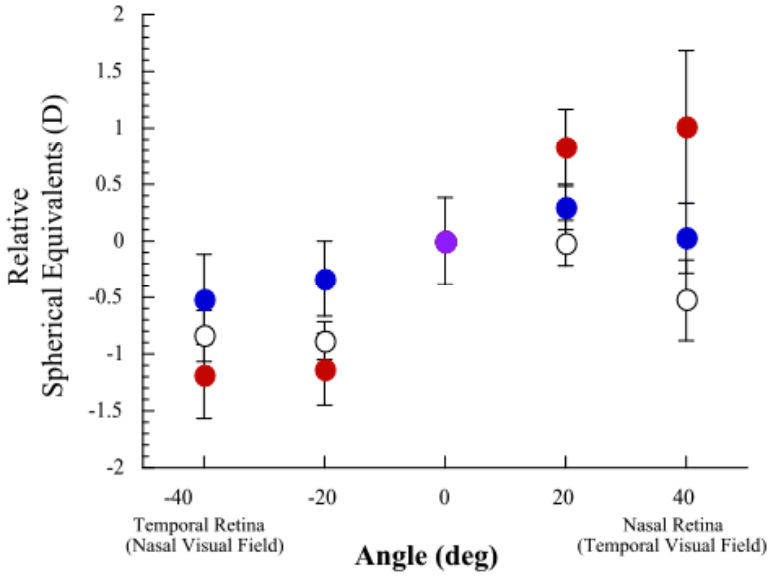
8b. Mean spherical equivalent error plotted as a function of horizontal eccentricity for control subjects. Black circles represent data from the right eye of controls. Grey circles represent data from the left eye of controls. Open circles represent data from both eyes of controls. Bars show standard error.

Figure 9

A.

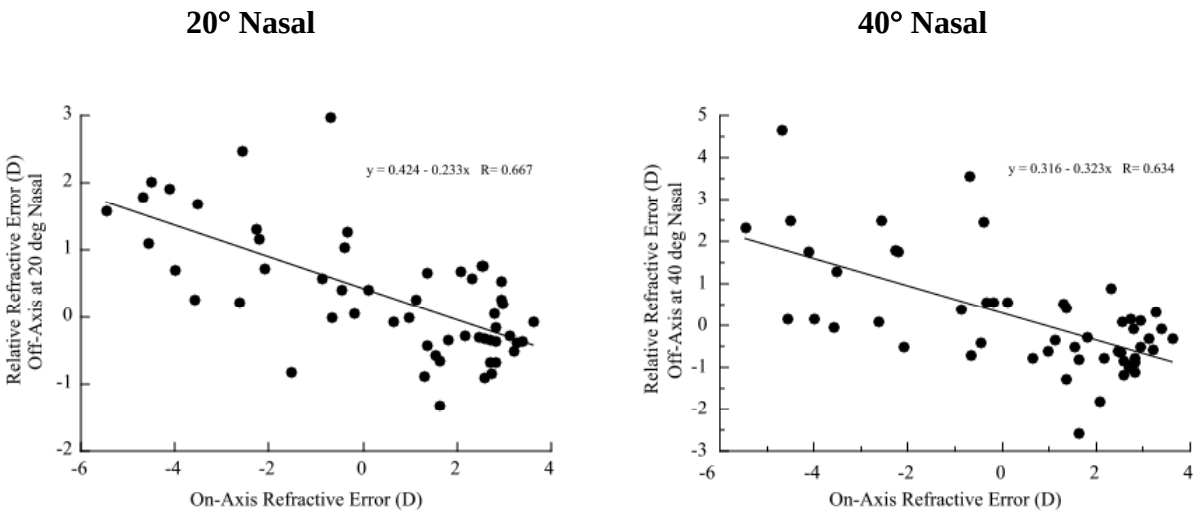


B.



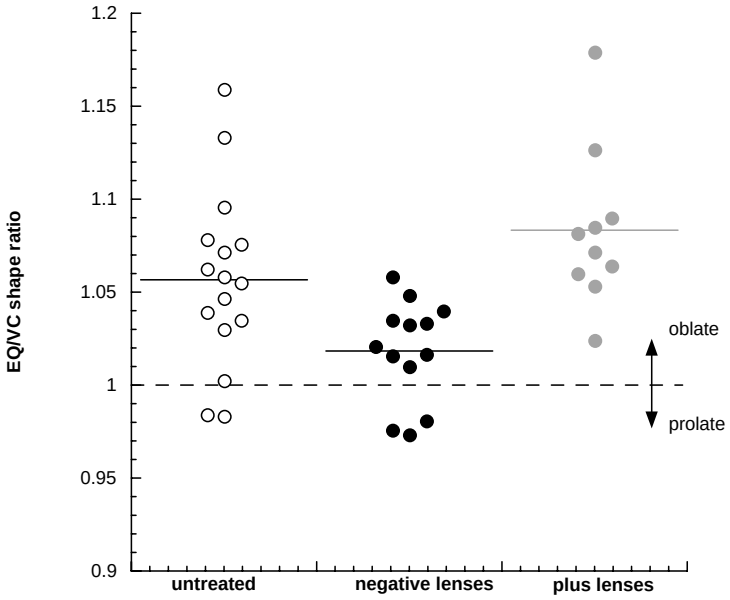
9. Relative spherical equivalent refraction plotted as a function of eccentricity along the horizontal meridian for binocular lens reared (**A**) and monocular lens reared (**B**) marmosets. All data are normalized to 0 D at 0° (purple circle). Relative refractive state in the nasal periphery of negative lens reared marmosets was significantly hyperopic in both binocular and monocular lens rearing paradigms (ANOVA, $p<0.01$).

Figure 10



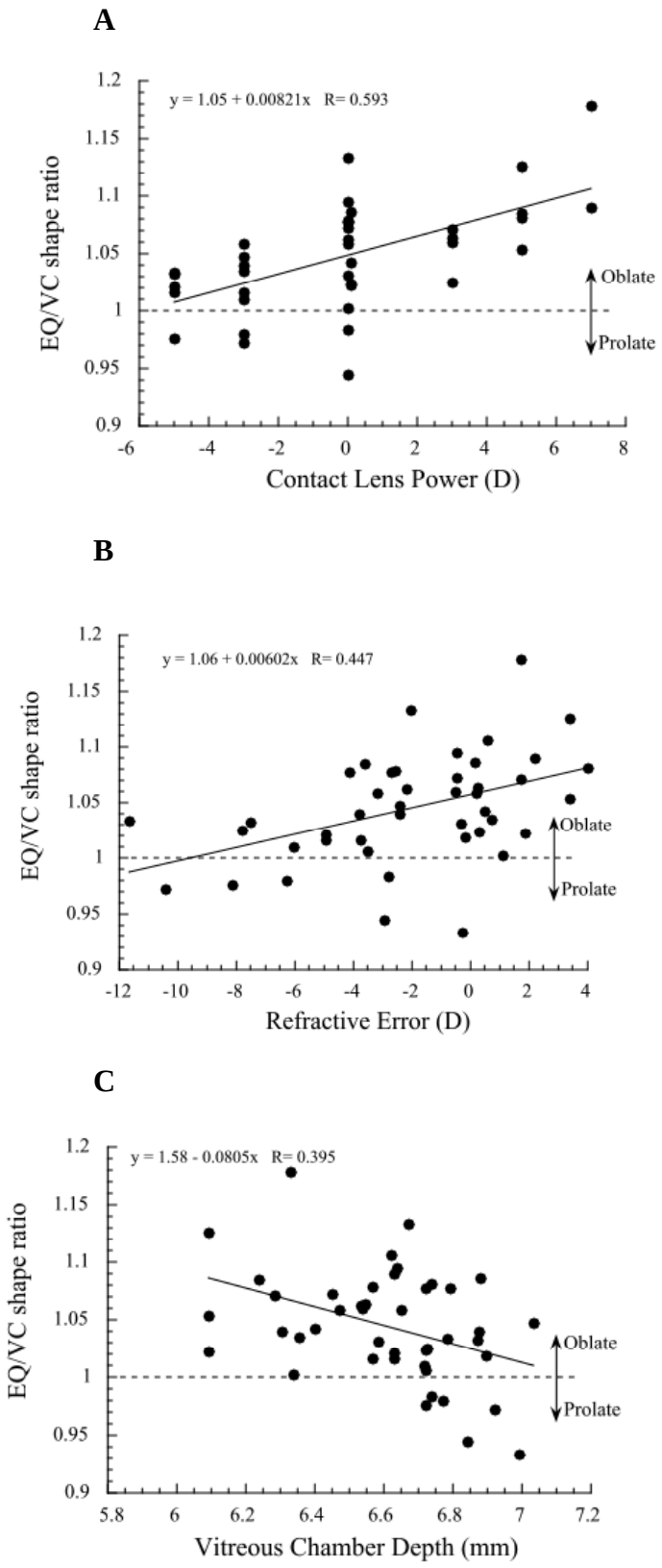
10. Peripheral spherical equivalent refractive state in minus lens reared marmosets along the nasal retina at 20° (left) and 40° (right) eccentricities was significantly correlated, and inversely proportional, to the refractive state measured on-axis.

Figure 11



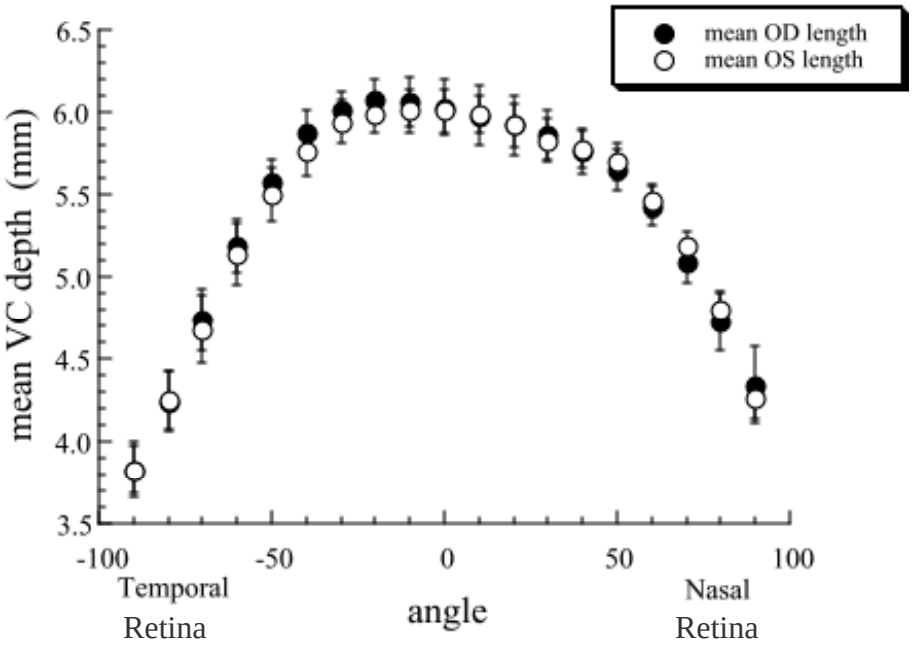
11. A plot of the EQ/VC shape ratio shows that marmoset eyes change shape during the development of induced axial refractive error. Relative to untreated controls (open circles) negative lens treated eyes (black circles) grew less oblate and in 3 cases more prolate, while all positive lens treated eyes (grey circles) had a reduction in vitreous chamber depth and became more oblate.

Figure 12



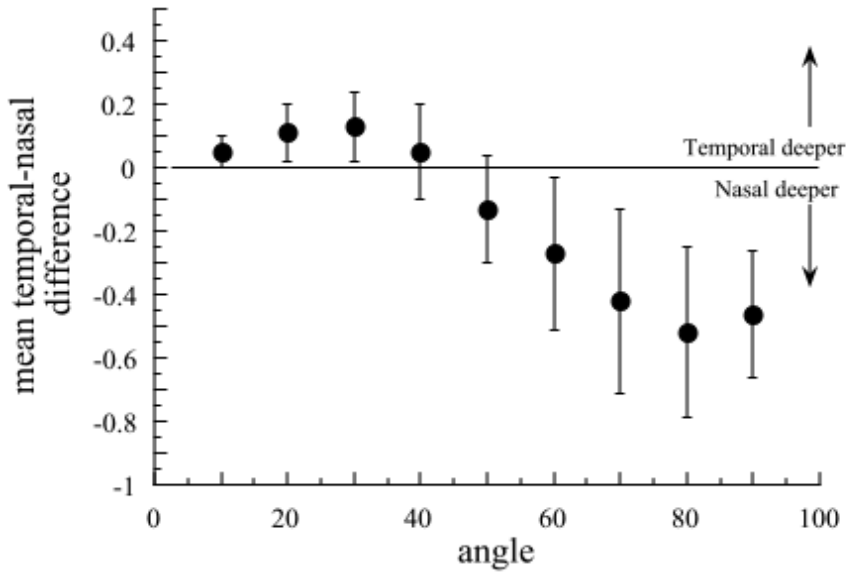
12. The equatorial diameter (EQ) to axial vitreous chamber depth (VC) shape ratio was significantly correlated with the power of lenses used (A), the degree of axial refractive error induced (B) and the axial vitreous chamber depth (C).

Figure 13
A



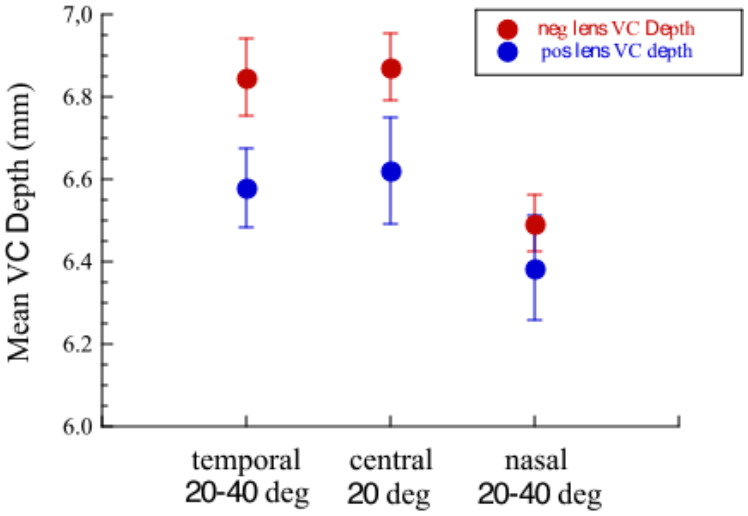
13a. Mean vitreous chamber depth measured along the horizontal plane in untreated control marmosets. Bars represent standard deviation. No significant difference was found between eyes.

Figure 13
B



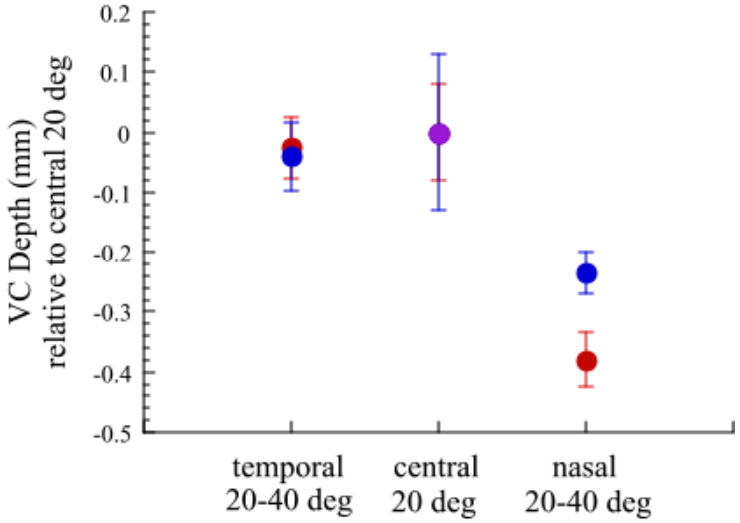
13b. Vitreous chamber depth varies with peripheral eccentricity in untreated eyes. A plot of the mean difference in vitreous chamber depth in temporal and nasal regions at corresponding angles suggests that the far periphery is deeper in the nasal retinal region than in the temporal retinal region.

Figure 14
A



14a. Mean vitreous chamber depth measured from MR images in negative lens treated eyes (red circles) and positive lens treated eyes (blue circles).

B



14b. Mean vitreous chamber depth relative to central 20 degrees measured from MR images in negative lens treated eyes (red circles) and positive lens treated eyes (blue circles).

DISCUSSION

Marmosets reared with soft-contact lenses that produce defocused retinal images, exhibit compensatory changes in refractive state and axial growth, confirming previous animals studies of emmetropization that suggest retinal defocus alters eye growth and refractive state (e.g. Diether & Schaeffel, 1997, Wallman et al., 1987; see Wallman & Winawer, 2004 for a review). The aim of this study was to establish our contact lens rearing paradigm in marmosets and then to investigate how imposed retinal defocus alters eye shape and peripheral refraction during the development of on-axis refractive error.

There were three main findings of the study: (1) soft-contact lens wear induced appropriate shifts in refractive state and axial growth, (2) peripheral refraction varied from central refractive state across the horizontal visual field, and (3) marmoset eyes changed shape during the development of axial refractive state in a way that was consistent with the observed peripheral refraction.

Positive lens wear imposed myopic blur, which resulted in significant shifts of hyperopic refractive state from reduced axial vitreous chamber depth, while negative lens wear imposed hyperopic blur resulting in myopic refractive state from induced axial vitreous chamber growth. Soft contact lens wear alone, had no effect on corneal power in any of the experimental groups, indicating that the induced refractive error is a result of changes in axial growth. Plano contact lenses had no effect on refractive state, vitreous chamber growth, or corneal power relative to untreated control eyes. There was, however, a response bias to negative lenses, where marmosets were found to compensate faster and greater to hyperopic defocus than to myopic defocus. One possible explanation may be that it takes the eye less

effort to compensate to negative lenses by inducing axial growth rather than what is needed to compensate to positive lenses with reduced axial growth (Ting, Schmid, Lam & Edwards, 2006; Troilo & Nickla, 2000; Troilo et al., 2009). Interestingly, marmosets reared binocularly with equal but opposite powered lenses had larger interocular compensatory responses than marmosets reared monocularly, suggesting that both lens rearing paradigms can be activated independently in both eyes (Troilo et al., 2009).

The second main finding was that peripheral refraction varied from central refractive state across the horizontal visual field. Myopic eyes were relatively hyperopic peripherally and hyperopic eyes were relatively myopic peripherally. Similar findings have been reported in both humans and infant macaque monkeys (Ferre et al., 1932; Rempt et al., 1971; Hoogerheide et al., 1971; Millodot 1981; Mutti et al., 2000; Atchison et al., 2006; Smith et al., 2005). In particular, the pattern of peripheral refraction in our minus lens reared myopic marmosets was similar to those reported in myopic humans, with the degree of relative peripheral hyperopia increasing with the degree of central myopia (Mutti et al., 2000; Atchinson et al. 2004). Whether peripheral refraction affects the development of axial refractive state or whether axial refraction affects peripheral refractive state remains unclear, but suggests that peripheral refraction should be considered when studying emmetropization.

The pattern of peripheral refraction varied with axial refractive state, but also exhibited a nasal-temporal asymmetry. Similar findings have also been found in infant macaque monkeys (Hung et al., 2008). Specifically, lens induced axial myopia was associated with significant relative hyperopia in the nasal periphery, but not in the temporal periphery. The finding of no significant differences between lens treated and control eyes in

the temporal retina suggest that specific retinal regions may be involved in the development of refractive state.

The third main finding of this project was that marmoset eyes changed shape during the development of axial refractive state in a way that was consistent with the observed changes in peripheral refraction. Control eyes were found to be relatively oblate in the horizontal plane. Hyperopic eyes were more oblate relative to control eyes, while myopic eyes were less oblate, and in some case prolate. Similar to the pattern of peripheral refractive state, eye shape varied along the horizontal plane with nasal-temporal asymmetry. Generally, myopic eyes were found to have shallower vitreous chamber depths on the nasal retina relative to the temporal retina, suggesting that the peripheral retinal grows asymmetrically, and contradicting the overall global enlargement proposed by Cheng et al., (1992). These findings are consistent with the posterior global shapes (Atchinson et al., 2004; Singh et al., 2006) and peripheral refractions (Hoogerheide 1971; Millodot 1974; Mutti et al, 2000) observed in human eyes. Although the MRI studies of human eye shape have conflicting results, it is generally agreed that human emmetropic and hyperopic eyes are oblate with relative peripheral myopia, whereas myopic eyes are prolate with relative peripheral hyperopia, and this is also true in the marmoset eye.

It has been suggested that in humans, variations in eye shape may be due to the anatomical constraint of orbit walls that restrict equatorial growth but allow for axial elongation (Mutti et al., 2000; Atchinson et al., 2004). A similar phenomenon may also be occurring in marmosets. MR images show that marmoset eyes are positioned close to the medial orbital wall, which may cause a restriction of equatorial growth, and further explain

the nasal-temporal asymmetries observed in the vitreous chamber depths of lens treated marmosets (Figure 15, below).

OD OS

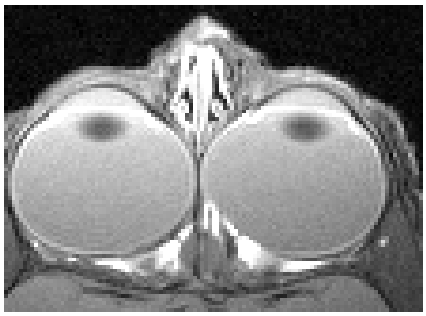


Figure 15. Example of MRI scan on a marmoset reared for fourteen weeks with a -3D lens (OD) and a +3D lens (OS). The close proximity of the medial orbital wall, in relation to the equator of the eye, may restrict equatorial growth and explain peripheral nasal-temporal asymmetries found in the vitreous chamber depths of lens treated eyes.

The eyes of macaque monkeys also appear restricted by the orbit walls and Huang et al. 2009, suggest that the anterior portions of the rectus muscles may further restrict equatorial growth. Thus, anatomical constraints may influence the eye shape changes observed in lens-reared marmosets.

Asymmetry in peripheral eye shape also corresponded to refractive state. Myopic marmoset eyes were found to be more hyperopic peripherally, but only on the nasal side of the retina, which also qualitatively corresponded to significantly reduced vitreous chamber depth in that region. A quantitative analysis, plotting a linear regression of eye shape to peripheral refractive state, awaits future study. If myopic prolate shaped eyes have significantly more hyperopia peripherally, then myopic individuals that continue to progress on-axis may consequently develop higher degrees of peripheral hyperopia. Another possibility is that the peripheral refractive state is influencing the development of axial refractive state and in turn causing changes in peripheral refraction and eye shape. In order

to determine whether peripheral defocus is a direct cause of axial refractive development, a follow-up study is needed where marmosets are reared with multifocal lenses that limit defocus to the periphery. If peripheral defocus is causing changes in axial refractive state, and if peripheral hyperopia causes axial myopia, then marmosets reared with lenses that have a plano central zone and a negative (hyperopic defocus) peripheral zone, would develop axial myopia. Accordingly, marmosets reared with lenses that have a plano central zone and a positive (myopic defocus) peripheral zone, would develop axial hyperopia. These results would confirm if peripheral defocus is the stimulus for regulation of axial eye growth and also have important clinical implications. In theory, myopic individuals could inhibit myopic progression by wearing lenses with peripheral hyperopia and a central myopic correction.

In addition to peripheral refraction influencing axial refraction, changes in eye shape may also be a predictive factor in determining who will develop axial myopia. Preliminary data from a longitudinal study of eye shape in Chinese school children suggests, for example, that differences in the shape ratio of equatorial diameter to the depth of vitreous chamber measured along the anterior-posterior axis are detected before changes in measures of axial vitreous chamber depth (Jiang, Totonelly, Zhou, Lu & Troilo, 2007). Jiang et al., 2007, measured eye shape from the MRIs of 34 Chinese children (mean age 11.6 years) and similar to reports using MRI on human adults (Atchinson et al., 2005), found a range of overall shapes with significant nasal-temporal and superior-inferior asymmetries. Generally, low myopic Chinese children had eyes that were prolate shaped (longer than wide). The possibility of correlating the rate of myopic progression with eye shape measures will

determine if shape is a risk factor for myopic development and whether it should be considered during traditional ocular examination.

In conclusion, peripheral retinal defocus and eye shape may influence axial refractive state by being a key factor in a visually growth dependent mechanism that regulates emmetropization. Additional studies of how the eye integrates signals of both axial and peripheral retinal defocus will help clarify the process of refractive development. Peripheral refraction, along with changes in eye shape, may help explain why some individuals become myopic and others do not. Further research is needed to determine how visually manipulating the peripheral retina alters axial refractive state.

References

Atchinson, D.A., Jones, C.E., Schmid, K.L., Pritchard, N., Pope, J.M., Strungell, W. E., and Riley, R.A. (2004). Eye shape in emmetropia and myopia. *Optometry and Vision Science*. 45, 3380-3386.

Atchison, D.A., Pritchard, N., & Schmid, K.L. (2006). Peripheral refraction along the horizontal and vertical visual fields in myopia. *Vision Research, 46* (8-9), 1450-1458.

Atchison, D.A., Pritchard, N., Schmid, K.L., Scott, D.H., Jones, C.E., & Pope, J.M. (2005). Shape of the retinal surface in emmetropia and myopia. *Investigative Ophthalmology and Vision Science, 46* (8), 2698-2707.

Baylor, E.R., & Shaw, E. (1962). Refractive error and vision in fishes. *Science, 136*, 157-158.

Boisvert, N., Wildsoet, C.F., & Troilo, D. (1998). Time course of cycloplegia in the marmoset: Relationship to mydriasis and the effect of anesthesia. *Optometry and Vision Science (Suppl.), 75* (12S), 265.

Chau, A., Fung, K., Pak, K., and Yap, M.(2004). Is eye shape related to orbit size in human subjects? *Ophthalmic and Physiological Opt*ics, 24, 35-40.

Chen, J.F., Elsner, A.E., Burns, S., Hansen, R.M., Lou, P.L, Kwong, K.K., & Fulton, A.B. (1992). The effect of eye shape on retinal responses. *Clinical Vision Sciences*, 7, 521-530.

Cheng, H.-M., Singh, O.S., Kwong, K.K., Xiong, J., Woods, B.T., & Brady, T.J. (1992). Shape of the myopic eye as seen with high resolution magnetic resonance imaging. *Optometry and Vision Science, 69*, 698-701.

Diether, S., & Schaeffel, F. (1997). Local changes in eye growth induced by imposed local refractive error despite active accommodation. *Vision Research, 37* (6), 659-668.

Dirani, M., Tong, L., Gazzard, G., Zhang, X., Chia, A., Young, T.L., Rose, K.A., Mitchell, P.R., and Saw, S-M. (2009). Outdoor activity and myopia in Singapore teenage children. *British Journal of Opthalmology*, 1-15.

Ferree, C.E., & Rand, G. (1933). Interpretation of refractive conditions in the peripheral field of vision: A further study. *Archives of Ophthalmology, 9*, 925-938.

Gilmartin, B., Logan, N., and Singh, K.D. (2007). Determining regional variations in globe conformation using 3-D ocular MRI. *Investigative Ophthalmology and Vision Science*, 49: E Abstract 3582.

Gilmartin, B., Logan, N., and Singh, K.D. (2008). In vivo comparison of anterior and posterior ocular volume in human ametropia. *Investigative Ophthalmology and Vision Science*, 48: E Abstract 1215.

Hammond, C.J., Sneider, H., Gilbert, C.E., Spector, T.D. (2001). Genes and environment in refractive error: the twin eye study. *Investigative Ophthalmology and Vision Science,* 42(6): 1232-1236.

Hepsen, I.F., Evereklioglu, C., & Bayramlar, H. (2001). The effect of reading and near-work on the development of myopia in emmetropic boys: a prospective, controlled, three-year follow-up study. *Vision Research, 41* (19), 2511-2520.

Hoogerheide, J., Rempt, F., & Hoogenboom, W.P.H. (1971). Acquired myopia in young pilots. *Ophthalmologica, 163*, 209-215.

Hung, L.-F., Crawford, M.L.J., & Smith, E.L. (1995). Spectacle lenses alter eye growth and the refractive status of young monkeys. *Nature Medicine, 1* (8), 761-765.

Hung, L.-F., & Smith III, E.L. (1996). Extended-wear, soft, contact lenses produce hyperopia in young monkeys. *Optometry and Vision Science*, *73* (9), 579-584.

Irving, E.L., Callender, M.G., & Sivak, J.G. (1991). Inducing myopia, hyperopia, and astigmatism in chicks. *Optometry and Vision Science, 68* (5), 364-368.

Ip, J.M., Saw, S-M., Rose, K., Morgan, I.G., Kifley, A., Wang, J.J., Mitchell, P. (2008). Role of Near Work in Myopia: Findings in a Sample of Australian School Children. *Investigative Ophthalmology and Vision Science,* 49 (7): 2903-2910.

Jiang, L., Totonelly, K., Zhou, X., Lu, F., & Troilo, D. (2007). Eye shape in Chinese school children measured by MRI – The Wenzhou Eye Shape Study. *Investigative Ophthalmology and Vision Science,* 49: E-Abstract 3144.

Jones LA, Sinnott LT, Mutti DO, Mitchell GL, Moeschberger ML, and Zadnik K. (2007). Parental history of myopia, sports, and outdoor activities, and future myopia. *Investigative Ophthalmology and Vision Science*, 48(8): 3524-3532.

Lin, L.L., Shih, Y.F., Hsaio, C.K., and Chen, C.J. (2004). Prevalence of myopia in Taiwanese school children: 1983 to 2000. *Annals Academy of Medicine Singapore, 33*: 27-33.

Llorente,L., Barbeo, S., Cano. D., Dorronsor. C., and Marcos, S. (2004). Myopic versus hyperopic eyes: axial length, corneal shape and optical aberrations. *Journal of Vision*, 4: 288-298.

Logan, N.S., Gilmartin, B., Wildoset, C.F., and Dunne, M.C. (2004) Posterior retinal contour in adult human anisomyopia. *Investigative Ophthalmology and Vision Science*, 45, 2152-2162

Lopes, M.C., Andrew, T., Carbonaro, F., Spector, T.D., and Hammond, C.J. (2009). Estimating heritability and shared environmental effects for refractive error in twin and family studies. *Investigative Ophthalmology and Vision Science,* 50(1): 126-131.

McBrien, N.A., & Norton, T.T. (1992). The development of experimental myopia and ocular component dimensions in monocularly lid-sutured tree shrews *(Tupaia belangeri). Vision Research, 32* (5), 843-852.

Miles, F.A., & Wallman, J. (1990). Local ocular compensation for imposed local refractive error. *Vision Research, 30* (3), 339-349.

Millodot, M. (1981). Effect of ametropia on peripheral refraction. *American Journal of Optometry and Physiological Optics, 58* (9), 691-695.

Millodot, M., & Lamont, A. (1974). Refraction in the periphery of the eye. *Journal of the Optical Society of America, 64* (1), 110-111.

Mutti, D.O., Hayes, J.R., Mitchell, G.L., Jones, L.A., Moeschberger, M.L., Cotter, S.A., Kleinstein, R.N., Manny, R.E., Twelker, J.D., & Zadnik, K. (2007). Refractive error, axial length, and relative peripheral refractive error before and after the onset of myopia. *Investigative Ophthalmology and Vision Science, 48* (6), 2510-2519.

Mutti, D.O., Sholtz, R.I., Friedman, N.E., & Zadnik, K. (2000). Peripheral refraction and ocular shape in children. *Investigative Ophthalmology and Vision Science, 41* (5), 1022-1030.

Norton, T.T., Essinger, J.A., & McBrien, N.A. (1994). Lid-suture myopia in tree shrews with retinal ganglion cell blockade. *Visual Neuroscience, 11* (1), 143-153.

Norton, T.T., Siegwart, J.T., Jr., & Amedo, A.O. (2006). Effectiveness of hyperopic defocus, minimal defocus, or myopic defocus in competition with a myopiagenic stimulus in tree shrew eyes. *Investigative Ophthalmology and Vision Science, 47* (11), 4687-4699.

Pacella, R., McLellan, J., Grice, K., Del Bono, E.A., Wiggs, J.L., Gwiazda, J.E. (1999). Role of genetic factors in the etiology of juvenile-onset myopia based on a longitudinal study of refractive error. *Optometry and Vision Science* 76(6), 442-448.

Raviola, E., & Wiesel, T.N. (1978). Effect of dark-rearing on experimental myopia in monkeys. *Investigative Ophthalmology and Vision Science, 17* (6), 485-488.

Rempt, F., Hoogerheide, J., & Hoogenboom, W.P.H. (1971). Peripheral retinoscopy and the skiagram. *Ophthalmologica,* 162, 1-10.

Schaeffel, F., Glasser, A., Howland, H.C. (1988). Accommodation, refractive error, and eye growth in chicks, *Vision Research,* 28 (5), 639-657.

Schaeffel, F., Simon,P., Feldkaemper,M., Ohngemach, S., Williams, R.W. (2003) Molecular biology of myopia. *Clinical and Experimental Optometry*. 86, 295-307.

Schippert, R., & Schaeffel, F. (2006). Peripheral defocus does not necessarily affect central refractive development. *Vision Research, 46*, 3935-3940.

Schmid, G.F., G.I. Papastergiou., Nickla D.L., Riva C.E., Lin T., Stone R.A., Laties A.M. (1996). Validation of laser Doppler interferometric measurements in vivo of axial eye length and thickness of fundus layers in chicks. *Current Eye Res*earch, 15, 691-696.

Seidemann, A., Schaeffel, F., Guirao, A., Lopez-Gil, N., & Artal, P. (2002). Peripheral refractive errors in myopic, emmetropic, and hyperopic young subjects. *Journal of the Optical Society of America. A, Optics Image Science and Vision, 19* (12), 2363-2373.

Sherman, S.M., Norton, T.T., & Casagrande, V.A. (1977). Myopia in the lid-sutured tree shrew *(Tupaia glis)*. *Brain Research*, *124*, 154-157.

Singh, K.D., Logan, N., and Gilmartin, B. (2004) Three Dimensional modeling of the human eye based on magnetic resonance imaging. *Investigative Ophthalmology and Vision Science*, 47, 2272-2279.

Smith III, E.L. & Hung, L-F. (1999). The role of optical defocus in regulating refractive development in infant monkeys. *Vision Research, 39,* 1415-1435.

Smith III, E.L., Bradley, D.V., Fernandes, A., & Boothe, R.G. (1999). Form deprivation myopia in adolescent monkeys. *Optometry and Vision Science, 76* (6), 428-431.

Smith III, E.L., Hung, L.F., & Harwerth, R.S. (1994). Effects of optically induced blur on the refractive status of young monkeys. *Vision Research, 34* (3), 293-301.

Smith III, E.L., Kee, C.S., Ramamirtham, R., Qiao-Grider, Y., & Hung, L.F. (2005). Peripheral vision can influence eye growth and refractive development in infant monkeys. *Invest. Opthalmol. Vis. Sci., 46* (11), 3965-3972.

Smith III, E.L., Huang, J., Hung, LF., Blasdel, T.L., Humbird, T.L., & Bockhorst, K.H. (2009). Hemiretinal form deprivation: evidence for local control of eye growth and refractive development in infant monkeys. *Investigative Ophthalmology and Vision Science,* 50 (11), 5057-5069.

Stone, R.A., and Flitcroff, D.I. (2004). Ocular shape and myopia. *Annals Academy of Medicine Singapore,* 33, 7-15.

Teikari, J.M., O'Donnell, J., ,Kaprio, J.,. Koskenvuo, M. (1991). Impact of heredity in myopia. *Human Heredity, 41*, 151-156.

Ting, P.W., Schmid, K.L., Lam, C.S., & Edwards, M.H. (2006). Objective real-time measurement of instrument myopia in microscopists under different viewing conditions. *Vision Research, 46* (15), 2354-2362.

Totonelly, K., & Troilo, D. (2008). Eye shape and off-axis refractive state following induced axial refractive errors in marmoset monkeys. *Investigative Ophthalmology and Vision Science, 49* : E-Abstract 1027.

Troilo, D., & Judge, S.J. (1993). Ocular development and visual deprivation myopia in the common marmoset *(Callithrix jacchus). Vision Research, 33* (10), 1311-1324.

Troilo, D., Judge, S.J., Ridley, R., & Baker, H. (1990). Myopia induced by brief visual deprivation in a New World primate – the common marmoset *(Callithrix jacchus). Investigative Ophthalmology and Vision Science (supplement), 31,* 1246.

Troilo, D., & Nickla, D.L. (2000). Visual regulation of eye growth and refractive state in a new world primate. In: F. Thorn, D. Troilo, & J. Gwiazda (Eds.), *Myopia 2000: Proceedings of the VIII International Conference on Myopia* (pp. 170-174). Boston, MA: Myopia 2000, Inc.

Troilo, D., Nickla, D.L., & Wildsoet, C.F. (2000a). Form deprivation myopia in mature common marmosets *(Callithrix jacchus). Investigative Ophthalmology and Vision Science, 41* (8), 2043-2049.

Troilo, D., Nickla, D.L., & Wildsoet, C.W. (2000b). Choroidal thickness changes during altered eye growth and refractive state in a primate. *Investigative Ophthalmology and Vision Science, 41* (6), 1249-1258.

Troilo, D., Totonelly, K & Harb, E. (2009). Imposed anisometropia, accommodation, and regulation of refractive state. *Optometry and Vision Science, 86* (1), E31-9.

Troilo, D., & Wallman, J. (1991). The regulation of eye growth and refractive state: an experimental study of emmetropization. *Vision Research*, 12: 133-153.

Vitale, S., Ellwein, L., Cotch, M.F., Ferris, F.L., and Sperduto, R. (2008). Prevalence of refractive error in the United States: 1999-2004. *Arch. Ophthalmol. 126,* 1111-1119.

Wallman, J. (1993). Retinal control of eye growth and refraction. In: Osborne, N., Chader, G. (Eds.), *Progress in Retinal Research, 12*. Pergamon Press, Oxford, pp. 133-153.

Wallman, J., Adams, J., & Trachtman, J.N. (1981). The eyes of young chickens grow toward emmetropia. *Investigative Ophthalmology and Vision Science, 20*, 557-561.

Wallman, J., & Adams, J.I. (1987). Developmental aspects of experimental myopia in chicks: Susceptibility, recovery and relation to emmetropization. *Vision Research, 27*, 1139-1163.

Wallman, J., Gottlieb, M.D., Rajaram, V., & Fugate-Wentzek, L. (1987). Local retinal regions control local eye growth and myopia. *Science, 237*, 73-77.

Wallman, J., Turkel, J., & Trachtman, J. (1978). Extreme myopia produced by modest change in early visual experience. *Science, 201*, 1249-1251.

Wallman, J., & Winawer, J. (2004). Homeostasis of eye growth and the question of myopia. *Neuron, 43*, 447-468.

Whatham, A.R., & Judge, S.J. (2001). Compensatory changes in eye growth and refraction induced by daily wear of soft contact lenses in young marmosets. *Vision Research, 41* (3), 267-273.

Whatham, A.R., and Judge, S.T. (2001). Overnight lens removal avoids changes in refraction and eye growth produced by plano soft contact lenses in infant marmosets. *Vision Research,* 41, 257-265.

Wiesel, T.N., & Raviola, E. (1977). Myopia and eye enlargement after neonatal lid fusion in monkeys. *Nature, 266*, 66-68.

Wildsoet, C., Wallman, J. 1995. Choroidal and scleral mechanisms of compensation for spectacle lenses in chicks. *Vision Research,* 35, 1175-1194.

Young, T.L. (2009). Molecular genetics of human myopia: an update. *Optometry and Vision Science,* 86(1): E8-E22.